Journal of Applied Polymer Science

Measurement of the Nonlinear Mechanical Properties of a Poly(vinyl alcohol) Sponge Under Longitudinal and Circumferential Loading

Alireza Karimi,[1,2] Mahdi Navidbakhsh[1,2]

[1]Tissue Engineering and Biological Systems Research Laboratory, School of Mechanical Engineering, Iran University of Science and Technology, Tehran 16844, Iran

[2]School of Mechanical Engineering, Iran University of Science and Technology, Tehran 16844, Iran

Correspondence to: M. Navidbakhsh (E-mail: mnavid@iust.ac.ir)

ABSTRACT: Poly(vinyl alcohol) sponges (P-sponges) have been used as a potential implant material for the replacement and repair of soft tissues, including cartilage, liver, and kidney. However, the application of P-sponges as tissue replacement materials is almost entirely bounded because of a lack of sufficient mechanical properties. In this study, we characterized the mechanical properties of a fabricated poly(vinyl alcohol) sponge (P-sponge) under a series of longitudinal and circumferential uniaxial loadings. The nonlinear mechanical behavior of the P-sponge was also computationally investigated with hyperelastic strain energy density functions, that is, the Ogden, Yeoh, Mooney–Rivlin, and Neo-Hookean models. A hyperelastic constitutive model was selected to best fit the axial behavior of the sponge. The results reveal that the Young's modulus and maximum stress of the P-sponge in the longitudinal direction were 16 and 17% greater than that in the circumferential direction, respectively. The Yeoh model, in addition, was selected to represent the nonlinear behavior of the poly(vinyl alcohol) material and could be used in future biomechanical simulations of the soft tissues. These results can be used to understand the mechanical properties of spongy materials in different loading directions. In addition, they have implications for ophthalmic and plastic surgeries and wound healing and tissue engineering purposes. © 2013 Wiley Periodicals, Inc. J. Appl. Polym. Sci. **2014**, *131*, 40257.

KEYWORDS: biocompatibility; biodegradable; bioengineering; biomedical applications; molding

Received 30 September 2013; accepted 4 December 2013

DOI: 10.1002/app.40257

INTRODUCTION

Poly(vinyl alcohol) sponges (P-sponges) are currently in widespread use for the removal and management of diffuse fluids/blood that are produced at or introduced to a surgical site.[1] They have also been contemplated as the most attractive biomedical polymers because of a combination of qualities, including biocompatibility,[2–5] high Hydrophilicity,[6–8] excellent mechanical strength and flexibility,[4–7,9,10] thermal stability and absence of toxicity,[11] availability, and relative cheapness.[12] These spongy materials may exhibit dissimilar mechanical behaviors in different loading directions because of their longitudinal and circumferential fibers. Their mechanical behaviors, such as their time-dependent viscoelastic behavior, is also similar to that of rubberlike materials. Thus, because of both the advantage of biocompatibility and the suitable mechanical properties of P-sponges, they can be used in the human body and in the pharmaceutical, and biomaterials areas,[13] for example, in tissue mimicking, vascular cell culturing, vascular implanting,[14] heart valves,[15] cartilage substitute,[6] contact lenses, and corneal implants.[6,10,16] One such application is the repair or replacement of wounded tissue, such as liver, kidney, or damaged articular cartilage. To treat them, several studies have been performed to use different materials in the replacement or repair of these tissues.[17] In this study, we aimed to design and conduct mechanical test setups to characterize the nonlinear mechanical behavior of P-sponges at two loading directions, including the longitudinal and circumferential directions, for potential use in the addition or substitution of native cartilage, liver, or kidney tissue scaffolds.

A critical barrier to the use of the P-sponge as tissue replacement material, however, is the lack of sufficient mechanical properties. This issue may contribute to the limited practical applications of P-sponges, and the most current usage of these sponges is as eye spears in ophthalmic, plastic, and hand surgeries. To overcome this problem, it is important to conduct sufficient tests for the nonlinear calibration and verification of suitable mathematical constitutive models under general axial states of stresses.[18] However, so far, most studies regarding the characterization of the mechanical properties of sponges for the purpose of tissue engineering have been concentrated on the

© 2013 Wiley Periodicals, Inc.

uniaxial mechanical properties.[19–21] The viscoelastic behavior of P-sponges can be important in the development of an implant that can replace the nucleus pulpous or any other soft tissues in the human body. Hence, the viscoelastic mechanical behavior of sponges is a key asset in its performance as a replacement tissue or as a scaffold in tissue engineering.[22] Fung's[23] quasi-linear viscoelastic (QLV) model has been used to describe the behavior of a large number of soft tissues.[24,25] It has the advantage that the required material functions can be obtained from relatively simple experiments. Furthermore, the substantial role of fibers on the longitudinal and circumferential mechanical properties of P-sponges has not been considered to date. Thus, it seems necessary to design a setup to measure the mechanical properties of P-sponges through the consideration of their viscoelastic and fiber mechanics effects.

In this study, we aimed to develop an experimental and analytical characterization of the nonlinear mechanical behavior of P-sponges under longitudinal and circumferential loading as candidates for the repair and replacement of the nucleus pulpous, damaged articular cartilage, liver, or kidney. Prony series were used in this study to characterize the viscoelastic part of the QLV model, and four independent hyperelastic models, including the Yeoh, Ogden, Mooney–Rivlin, and Neo-Hookean models, were implemented for the elastic response. Prony series have been widely used to adjust the viscoelastic behavior of many soft tissues.[26,27] The proposed hyperelastic models were calibrated from the experimental results and used to predict the mechanical response of the sponge under general axial stress states.

EXPERIMENTAL

Materials and Specimen Preparation

To prepare a poly(vinyl alcohol) (PVA) aqueous solution, 2 g of PVA (molecular weight = 40,000, Sigma-Aldrich) was dissolved in 100 mL of distilled water at 50°C under stirring at 400 rpm for 6 h. The polymer solution was then cast into cylindrical molds and freeze-dried to obtain the PVA spongy matrix. To improve its stability in water, this sponge was crosslinked by exposure to the vapors of a glutaraldehyde aqueous solution (25%) at 37°C for 24 h. After it was rinsed with distilled water, the sponge was freeze-dried again. The crosslinking procedure varied slightly, depending on the crosslinking density desired for each experiment.The crosslinking ratio (X), expressed in moles of glutaraldehyde per mole of PVA repeating units, was calculated; this ratio varied between 0.01 and 0.20. In a typical procedure for the preparation of gels with X = 0.10, the following aqueous reagents were sequentially added to the PVA solution, with stirring: 2.0 mL of 50 vol % of methanol, 3.0 mL of 10 vol % of acetic acid, 1.9 mL of 25 vol % of glutaraldehyde, and 1.0 mL of 1 vol % of sulfuric acid. The final solution was poured into Petri dishes and allowed to stand at room temperature (25–30°C) until crosslinking was completed (48 h).

Axial and Lateral Measurements

The samples were divided into two groups; including samples with longitudinal and circumferential fibers. It should be noted that during the longitudinal uniaxial loading, the longitudinal fibers and, during the circumferential loading, the circumferential fibers came to act. The initial dimensions of all of the specimens were measured precisely. The tensile test was performed with a uniaxial tensile test apparatus adapted for testing the biological specimens used in our previous studies.[28,29] All tests were performed at 25°C, and each sample was tested only once. A low strain rate of 5 mm/min, which is typical for surgical procedures, and this gave us more insight into how tissue behavior was employed by the action of an axial servo motor.[30] It has also been recommended that a slow strain rate should be used in stress-relaxation tests[31,32] because, at a low strain rate, the actual strain history can be approximated well by a linear ramp followed by holding at constant strain. To ensure the firm fixation of the samples between the jaws of the machine, a small tensile preload of 0.05 N was applied to each specimen. Moreover, rough sandpaper was used between the jaw and sample to ensure that there were no slip boundaries. The sample's length was measured after the application of the preload. This also helped minimize the bending effect caused by the weight of each specimen.

Stress Relaxation Testing

Stress relaxation testing was performed with the uniaxial tensile testing machine at two different loading directions. The load limits were predetermined by the linear portion of the stress–strain curves obtained previously under uniaxial tensile testing. The samples were subjected to a constant-step tensile strain applied at a rate of 5 mm/min, and the sample was allowed to relax for 330 s.

Constitutive Equations: Strain Energy Density Functions (SEDFs)

The confined and unconfined experimental data was used to calibrate an isotropic hyperelastic SEDF to generate multiaxial stress–strain relations that could be used in finite-element simulation of sponges. Under the assumption that sponge is an isotropic material, it was possible to fit a general polynomial isotropic SEDF form [eq. (1)]. Four different isotropic SEDF models were examined: Yeoh [eq. (2)], Ogden [eq. (3)], Mooney–Rivlin [eq. (4)], and Neo-Hookean [eq. (5)]. The Yeoh, Mooney–Rivlin,[33] and Neo-Hookean[34] models are special cases of polynomial SEDFs, whereas the Ogden[35] model can be also considered as a polynomial form in terms of the stretch ratios as its variables instead of the invariants. The polynomial, along with the other specialized forms of the SEDFs, can be written as follows:

$$W=\sum_{i+j=1}^{N} C_{ij}(\bar{I}_1-3)^i(\bar{I}_2-3)^j + \sum_{i=1}^{N}\frac{1}{D_i}(J-1)^{2i} \mid i,j=0,1,\ldots,N \mid i+j=1,2,\ldots,N \quad (1)$$

$$W=\sum_{i=1}^{3} C_{i0}(\bar{I}_1-3)^i+\sum_{i=1}^{N}\frac{1}{D_i}(J-1)^{2i} \quad (2)$$

$$W=\sum_{i=1}^{N}\frac{\mu_i}{\alpha_i}(\bar{\lambda}_1^{\alpha_i}+\bar{\lambda}_2^{\alpha_i}+\bar{\lambda}_3^{\alpha_i}-3)+\sum_{i=1}^{N}\frac{1}{D_i}(J-1)^{2i} \quad (3)$$

$$W = C_{10}(\bar{I}_1 - 3) + C_{01}(\bar{I}_2 - 3) + \frac{1}{D_1}(J-1)^2 \quad (4)$$

$$W = C_{10}(\bar{I}_1 - 3) + \frac{1}{D_1}(J-1)^2 \quad (5)$$

where W is strain energy density function and D_i is a volumetric coefficient, $J = \det(F)$ and F is the deformation gradient. $\bar{I}_1$ and $\bar{I}_2$ are the first and second invariants, respectively, of the left Cauchy–Green strain tensor (**B**). For the normalized deformation gradient ($\bar{F} = J^{-1/3}F$), **B** assumes the following form: $\mathbf{B} = \bar{F}\bar{F}^T$. The principle stretch ($\bar{\lambda}_i$) is the eigenvalue of $\bar{F}$. The polynomial coefficients μ_i, α_i, and C_{ij} are material constants that were fit from the experimental data.

It should be noted that the previous SEDFs were composed of two sums. The first was related to the uncompressive part of the function with the first and second invariants, whereas the second sum was for the compressive part of the SEDF with the third strain invariant. Linear least squares fit was used for the Mooney–Rivlin, Neo-Hookean, and Yeoh model calibration, and nonlinear least squares fit was applied to match the constant for the Ogden model.

QLV Model

A material is said to be viscoelastic if the material has an elastic (recoverable) part and a viscous (nonrecoverable) part. Upon application of a load, the elastic deformation is instantaneous, whereas the viscous part occurs over time. The QLV model, first proposed by Fung,[36,37] is commonly used to characterize soft biological tissues.[38–40] The QLV formulation captures the well-established elastic nonlinearities of soft tissues.

In Fung's approach, the history of the stress response, called the *relaxation function* $[\sigma(\lambda,t)]$ is factorized that uses a normalized function of time, called the reduced relaxation function $[G(t)]$, and a function of the stretch (λ), called the *elastic response* $[T^{(e)}]$. If a tensile stretch (or shortening) is applied on a cylindrical specimen as a step function, the stress developed is given by the following model:

$$\sigma(\lambda, t) = G(t)\,T^{(e)}(\lambda),\ G(0) = 1 \quad (6)$$

where T is a transpose of matrix, $T^{(e)}$ represents the Cauchy stress that would be produced if no relaxation has taken place.

It was assumed that the stress response to changes in the stretch could be evaluated with the Boltzmann superposition principle, and if the specimen was stress- and strain-free at time $t = 0$, the stress $[\sigma(t)]$ could be expressed as follows:

$$\sigma(t) = \int_0^t G(t-\tau)\frac{\partial T^e(s)}{\partial \lambda}\frac{\partial \lambda(\tau)}{\partial \tau}\partial\tau + \sigma_0 \quad (7)$$

If $G(t)$ is assumed to be continuously differentiable, the expression can also be written as follows:

$$\sigma(t) = T^e[\lambda(t)] + \int_0^t T^e[\lambda(t-\tau)]\frac{\partial G(\tau)}{\partial \tau}\partial\tau \quad (8)$$

For this study, $G(t)$ was approximated by the Prony series:[41,42]

$$G(t) = G_\infty + \sum_{i=1}^{3} G_i e^{\frac{-t}{\tau}} \quad (9)$$

Subjected to the constraint

$$G_0 = G_\infty + G_1 + G_2 + G_3 = 1 \quad (10)$$

Where G_∞ is the long-term relaxation coefficient [$G_\infty = \lim_{t\to\infty} G(t)$] and the G_i coefficients indicate the relaxation strength corresponding to the τ_i time constant. Successive time constants were incrementally increased by decade values,[39,41] ending at the decade value that corresponded to the length of the experiment: $\tau_1 = 60$ s, which was chosen to temporally coincide with the experimental ramp time (<60 s), where $\tau_2 = 150$ s and $\tau_3 = 300$ s.

The instantaneous elastic stress and its derivative are represented by nonlinear equations:

$$\sigma^e(\varepsilon) = A(e^{B\varepsilon} - 1) \quad (11)$$

$$\frac{\partial \sigma^e(\varepsilon)}{\partial \varepsilon} = ABe^{B\varepsilon} \quad (12)$$

where $\sigma^e(\varepsilon)$ is a elastic stress, $e^{B\varepsilon}$ is A and B in equ. 11 and 12 are defined. e is that equations is defined as mathematical constant (=2.718), A and B are the instantaneous elastic parameters,[39,42,43] which can be calibrated by the fitting of the experimental data.

If the applied ramp history is complex (not a pure linear ramp and constant hold), differentiation of the applied strain history makes eq. (6) difficult to directly implement by numerical integration. Therefore, to simplify the integration of eq. (6) for this study, the differential operator was removed from the input strain history via integration by parts:

$$\sigma(\varepsilon, t) = ABe^{B\varepsilon}\left[-\int_0^t \frac{dG(t-\tau)}{d\tau}\varepsilon(\tau)d\tau + G(t-\tau)\varepsilon(t) - G(t-0)\varepsilon(0)\right] + \sigma_0 \quad (13)$$

where τ is a time constant or characteristic time, ε is defined a strain, σ_0 equals to initial stress, $\varepsilon(0)$ is a strain function at its initial condition.

The typical QLV stress relaxation curve fit with the Abramowitch and Woo[32] method was used for this study. The values of the reduced relaxation coefficients were then obtained with MATLAB version R2010a (The MathWorks, Inc., Natick, MA). The average coefficient of determination (R^2) was calculated between the model and experimental results for each specimen.

Swelling Analysis

To estimate the swelling behavior of the P-sponges, the prepared samples were immersed in phosphate-buffered saline at room temperature, which is commonly chosen as the swelling medium for swelling analysis. During the swelling process, the mass of the samples was weighed periodically until the swelling behavior of the PVA reached the equilibrium stage.[2] Four independent samples were tested ($n = 4$), and the swelling ratio (SR) was calculated with the following method:

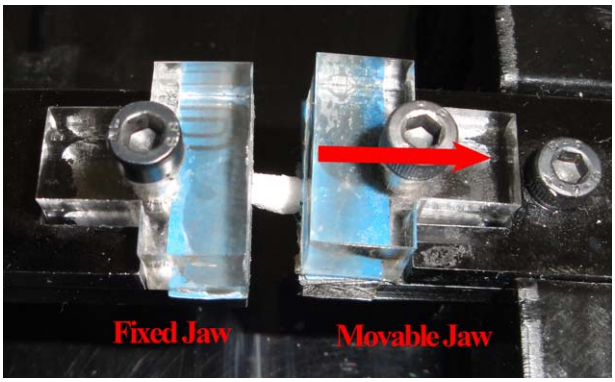

Figure 1. P-sponges during tensile testing. [Color figure can be viewed in the online issue, which is available at wileyonlinelibrary.com.]

$$SR = \frac{W_i - W_d}{W_d} \times 100 \quad (14)$$

where W_i is the weight of the sample at various times and W_d is the weight of the sponge in the dry state.[7,44]

Statistical Analysis

The data were first analyzed by analysis of variance; when statistical differences were detected, a student's t test for comparisons between groups was performed with SPSS software version 16.0 (SPSS, Inc., Chicago, IL). The data are reported as the mean plus or minus the standard deviation at a significance level of $p < 0.05$.

RESULTS AND DISCUSSION

Although P-sponges possess many attractive features for biomedical applications, the mechanical properties of these versatile biomaterials are generally poor.[45] The mechanical testing of P-sponges is, therefore, an important part of a comprehensive evaluation for load-bearing applications, and the chosen methodology should be directly relevant to the intended functional loading conditions.[6] Many authors have used linear viscoelasticity to relate the stress and strain using the Voigt, Maxwell, and Kelvin models for different soft tissues.[46–48] However, for large displacements and/or strains, these models might not be valid, and the nonlinear stress–strain characteristics of these tissues must be considered.[23] With that in mind, the purpose of this study was to quantify the longitudinal and circumferential hyperviscoelastic mechanical properties of a PVA biomaterial intended for use as an eye spear in ophthalmic surgical procedures and as an implant for tissue engineering purposes.

A PVA specimen during uniaxial testing is illustrated in Figure 1. The uniaxial tensile test machine was consisted a fixed and moveable jaw, which provided us with a constant strain rate. Samples were tested in the longitudinal (y) and circumferential (x) directions to consider the effects of the fiber direction on the mechanical properties (Figure 2). P-sponges, like other spongy materials, consist of fiber networks. It should be noted that during the longitudinal uniaxial loading, the longitudinal fibers and, during the circumferential loading, the circumferential fibers came to act (Figure 3). The stress–strain diagram for the P-sponge under longitudinal and circumferential loadings is indicated in Figure 4. The Young's moduli of the P-sponge in the longitudinal and circumferential directions were 38.91 and

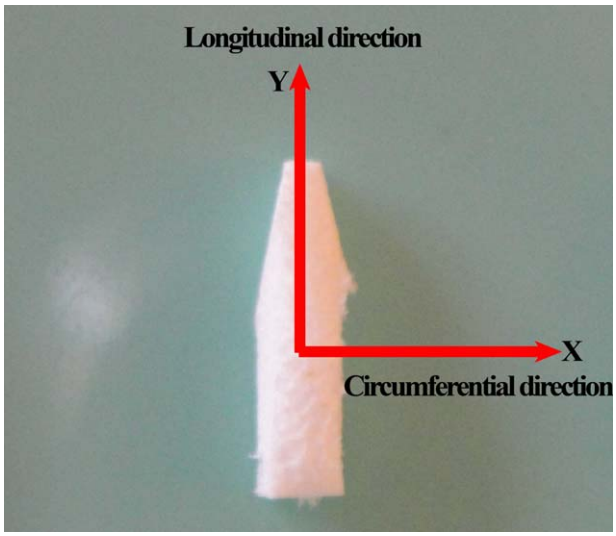

Figure 2. P-sponge along the two loading directions: longitudinal (y) and circumferential (x). [Color figure can be viewed in the online issue, which is available at wileyonlinelibrary.com.]

33.34 MPa, respectively. The maximum stress in the longitudinal direction was 17.90% greater than that in the circumferential direction (Figure 5). However, there was no considerable variation in the longitudinal and circumferential directions for the maximum strain (5.11%). The results from the tensile experimental tests were used to calibrate the SEDF candidates used for axial constitutive modeling. The experimental data were used to fit the incompressible part of the SEDF, whereas the confined data were applied in the fitting of the compressive part of the SEDF. Material constants for each SEDF candidate are listed in Tables I and II. The plotted representative test result was the average values generated from all of the samples at their last loading cycle. Different ranges of ability to match the test results were demonstrated by these functions. For example, the lack of the second variable in the Neo-Hookean SEDF impaired it to a lower bound and larger error. The Neo-

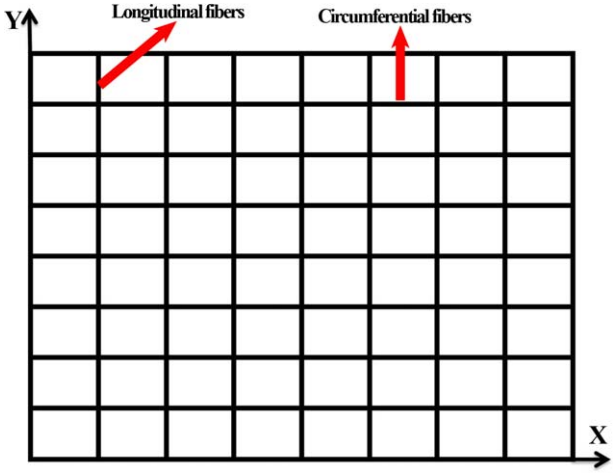

Figure 3. Longitudinal (y) and circumferential (x) fibers for the P-sponge. [Color figure can be viewed in the online issue, which is available at wileyonlinelibrary.com.]

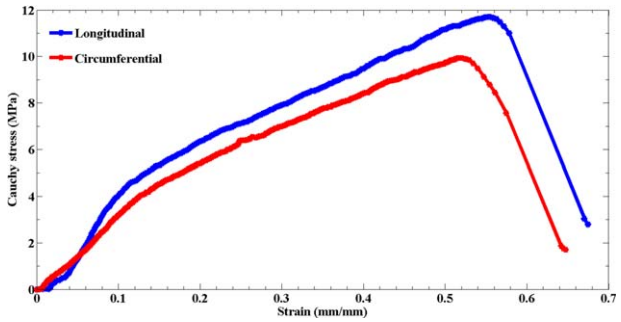

Figure 4. Experimental stress–strain diagrams of the P-sponge for both the longitudinal and circumferential directions. [Color figure can be viewed in the online issue, which is available at wileyonlinelibrary.com.]

Hookean function failed to capture the nonlinear behavior of the P-sponge under uniaxial stress states. The Ogden and Mooney–Rivlin SEDFs showed similar behavior and adequate ability to predict the sponge behavior for most of the test data range. They diverged from the Yeoh model at larger uniaxial strain magnitudes. The Yeoh SEDF showed excellent ability to model the stress–strain data for the entire range. The Yeoh and Ogden SEDFs showed a very close response and matched the entire range of the test data. The Yeoh and Ogden SEDFs demonstrated good matching with the tensile test results.[19,20] The aim was to select a constitutive hyperelastic model for the P-sponge under service conditions with a high water content. Therefore, the Yeoh and Ogden functions seemed to be more logical selections to represent its behavior where incompressible behavior was expected for higher hydrostatic stretch values.

The stress versus time curves were plotted according to the obtained mechanical data (Figure 6). There was no significant difference on the ramp section of the relaxation curves. This indicated that the viscoelastic behavior of the P-sponge in both the longitudinal and circumferential directions did not vary significantly. The elastic modulus was the slope of the line fitted to the entire quasi-linear domain of these curves.[7,49] The results

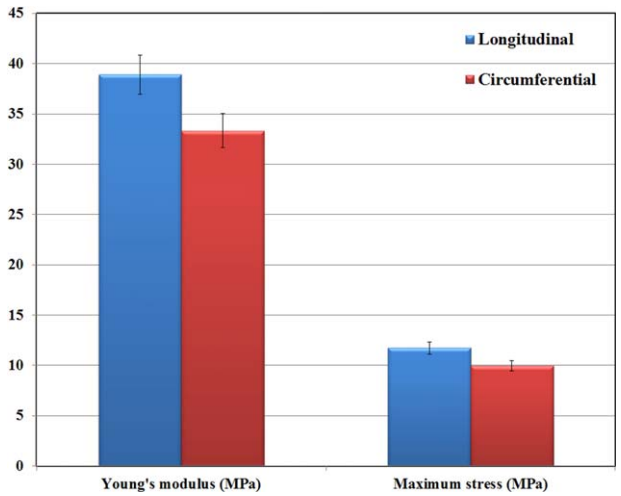

Figure 5. Young's modulus and maximum stress of the P-sponge in the longitudinal and circumferential directions. [Color figure can be viewed in the online issue, which is available at wileyonlinelibrary.com.]

Table I. Material Constants for the P-Sponges in the Longitudinal Direction

	Material constant (MPa)			
Hyperelastic model	C_{10}	C_{01}	C_{20}	C_{30}
Mooney–Rivlin	8.27	−3.97	-	-
Neo-Hookean	0.14	-	-	-
Yeoh	0.07	-	17.49	−14.93
Hyperelastic model	μ_1	μ_2	α_1	α_2
Ogden	498.25	−499.04	−1.25	−1.89

Table II. Material Constants for the P-Sponges in the Circumferential Direction

	Material constant (MPa)			
Hyperelastic model	C_{10}	C_{01}	C_{20}	C_{30}
Mooney–Rivlin	2.41	3.32	-	-
Neo-Hookean	2.62	-	-	-
Yeoh	1.42	-	12.96	−12.61
Hyperelastic model	μ_1	μ_2	α_1	α_2
Ogden	38.33	−37.27	2.91	−10.49

show that the maximum stress before the holding (at 60 s) in the longitudinal direction was 12.5% higher than that in the circumferential direction. Biomaterials for tissue engineering applications require the tight control of a number of properties, including the mechanical stiffness, physical integrity, and bearing load, until they are replaced by newly formed tissues.[50] An ideal implant, thus, should have physical and mechanical properties that are as close as possible to those of the tissues being replaced. For instance, sutures and stents that provide mechanical support for wounded tissues should possess appropriate mechanical properties, such as strength, stiffness, and ductility (extensibility).[51,52] Interestingly, the material behavior under stress relaxation for the ramping portion of synthetic matrices (concave downward) was opposite to that of soft tissues (concave upward), such as ligaments and tendons.[53,54] The values of A (0.16 and 0.19 MPa for the longitudinal and circumferential directions, respectively) and B (2.05 and 1.88 MPa for the

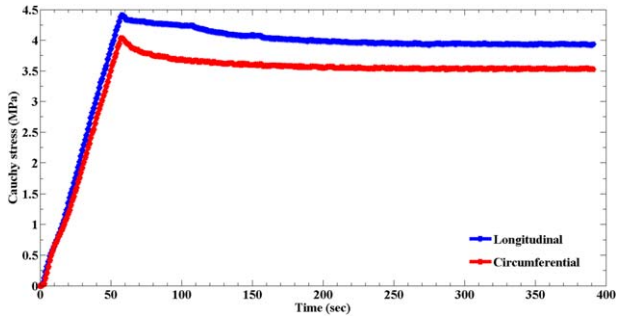

Figure 6. Relaxation diagram of the P-sponge in the longitudinal and circumferential directions. [Color figure can be viewed in the online issue, which is available at wileyonlinelibrary.com.]

Table III. Identified Parameters of the QLV Material Model for the P-Sponges

P-Sponge	Longitudinal	Circumferential
G_∞	0.18 ± 0.03	0.16 ± 0.03
G_1	0.42 ± 0.08	0.39 ± 0.06
G_2	0.11 ± 0.02	0.16 ± 0.04
G_3	0.28 ± 0.07	0.23 ± 0.05
A (MPa)	0.16 ± 0.01	0.19 ± 0.04
B	2.05 ± 0.10	1.88 ± 0.10
R_2	0.97	0.96

longitudinal and circumferential directions, respectively; Table III), the constants of the elastic stress response function, were found to be in a different range in comparison to those in other tissues, including soft ones.[55,56] An efficient solution would be to find an alternative biological counterpart for those materials in use. The strain rate was also considered to be an independent factor that had no influence on the results.[6]

Swelling analysis also revealed that the P-sponge had a very high swelling capacity and the ability to retain water in excess of its original weight (>14 times its original weight),[19,20] and this was a considerable appropriate factor for the purpose of ophthalmic and plastic surgeries. Sionkowska et al.,[57] however, showed that the greatest degree of swelling was attributed to sponge made of silk fibroin, which had a swelling degree of almost 1600%, which was much higher than that of chitosan, which was 1200%.

CONCLUSIONS

In this study, we investigated the mechanical properties of a P-sponge with a uniaxial tensile test instrument at two different loading directions, the longitudinal and circumferential directions. The findings reveal that the P-sponge showed dissimilar mechanical properties in different loading directions. We believe that the following differences were related to the fiber orientations, whose actions depended on the loading direction. The viscoelastic behavior of the P-sponge, however, indicated no significant variation. We also presented a modified QLV model to predict the response of biodegradable polymers; it was subject to mechanical loading, which is suitable for applications in biodegradable biomaterials. This would provide a new P-sponge use in other fields of biomedical and biomaterial applications. PVA material may be a suitable substitute for creatural soft tissue in investigations of soft tissue deformation for biopsy precision research.

ACKNOWLEDGMENTS

The authors acknowledge the Iran University of Science and Technology for funding this project.

REFERENCES

1. Korteweg, W.; Korteweg, G. P. U.S. Pat. 006711879B2 (**2004**).
2. Shi, Y.; Xiong, D. *Wear* **2013**, *305*, 280.
3. DiTizio, V.; Ferguson, G. W.; Mittelman, M. W.; Khoury, A. E.; Bruce, A. W.; DiCosmo, F. *Biomaterials* **1998**, *19*, 1877.
4. Zhang, D.; Chen, K.; Wu, L.; Wang, D.; Ge, S. *J. Bionic Eng.* **2012**, *9*, 234.
5. Lee, S.-Y.; Pereira, B. P.; Yusof, N.; Selvaratnam, L.; Yu, Z.; Abbas, A. A.; Kamarul, T. *Acta Biomater.* **2009**, *5*, 1919.
6. Stammen, J. A.; Williams, S.; Ku, D. N.; Guldberg, R. E. *Biomaterials* **2001**, *22*, 799.
7. Lee, C.-T.; Kung, P.-H.; Lee, Y.-D. *Carbohydr. Polym.* **2005**, *61*, 348.
8. Setiawan, L.; Wang, R.; Li, K.; Fane, A. G. *J. Membr. Sci.* **2012**, *394*, 80.
9. Young, C.-D.; Wu, J-R.; Tsou, T.-L. *Biomaterials* **1998**, *19*, 1745.
10. Kobayashi, H.; Kato, M.; Taguchi, T.; Ikoma, T.; Miyashita, H.; Shimmura, S.; Tsubota, K.; Tanaka, J. *Mater. Sci. Eng. C* **2004**, *24*, 729.
11. Liu, L.; Zhao, C.; Yang, F. *Water Res.* **2012**, *46*, 1969.
12. Moscato, S.; Mattii, L.; D'Alessandro, D.; Cascone, M. G.; Lazzeri, L.; Serino, L. P.; Dolfi, A. *Micron* **2008**, *39*, 569.
13. Liu, Y.; Geever, L. M.; Kennedy, J. E.; Higginbotham, C. L.; Cahill, P. A.McGuinness, G. B. *J. Mech. Behav. Biomed. Mater.* **2010**, *3*, 203.
14. Jiang, S.; Liu, S.; Feng, W. *J. Mech. Behav. Biomed. Mater.* **2011**, *4*, 1228.
15. Jiang, H.; Campbell, G.; Boughner, D.; Wan, W-K.; Quantz, M. *Med. Eng. Phys.* **2004**, *26*, 269.
16. Vijayasekaran, S.; Fitton, J. H.; Hicks, C. R.; Chirila, T. V.; Crawford, G. J.; Constable, I. *J. Biomaterials* **1998**, *19*, 2255.
17. Sebastine, I, M.; Williams, D. J.29th Annual International Conference of the IEEE EMBS. **2007**, *23*.
18. Anseth, K. S.; Bowman, C. N.; Brannon-Peppas, L. *Biomaterials* **1996**, *17*, 1647.
19. Karimi, A.; Navidbakhsh, M.; Faghihi, S. *Perfusion*, to appear.
20. Karimi, A.; Navidbakhsh, M. *Mater. Technol. Adv. Perform. Mater.* doi: 10.1179/1753555713Y.0000000115.
21. Karimi, A.; Navidbakhsh, M.; Faghihi, S. *J. Biomater. Tissue Eng.* **2014**, *4*, 46.
22. Tanaka, E.; Tanaka, M.; Aoyama, J.; Watanabe, M.; Hattori, Y.; Asai, D.; Iwabe, T.; Sasaki, A.; Sugiyama, M.; Tanne, K. *Arch. Oral Biol.* **2002**, *47*, 139.
23. Fung, Y. Biomechanics: Mechanical Properties of Living Tissues; Springer-Verlag: New York, **1993**.
24. Carew, E.; Talman, E.; Boughner, D.; Vesely, I. *J. Biomech. Eng.* **1999**, *121*, 386.
25. Drapaca, C.; Tenti, G.; Rohlf, K.; Sivaloganathan, S. *J. Elast.* **2006**, *85*, 65.
26. Laksari, K.; Shafieian, M.; Darvish, K. *J. Biomech.* **2012**, *45*, 642.
27. Lamela, M.; Prado, Y.; Fernandez, P.; Fernández-Canteli, A.; Tanaka, E. *Exp. Mech.* **2011**, *51*, 1453.
28. Karimi, A.; Navidbakhsh, M.; Shojaei, A.; Faghihi, S. *Mater. Sci. Eng. C* **2013**, *33*, 2550.

29. Karimi, A.; Navidbakhsh, M.; Faghihi, S.; Shojaei, A.; Hassani, K. *Proc. IMechE Part H: J. Eng. Med.* **2013**, *227*, 148.
30. Karimi, A.; Navidbakhsh, M.; Haghi, A. M.; Faghihi, S. *Proc. IMechE Part H: J. Eng. Med.* **2013**, *227*, 609.
31. Gimbel, J. A.; Sarver, J. J.; Soslowsky, L. J. *J. Biomech. Eng.* **2005**, *126*, 844
32. Abramowitch, S.; Woo, S. *J. Biomech. Eng.* **2004**, *126*, 92.
33. Karimi, A.; Navidbakhsh, M.; Shojaei, A.; Hassani, K.; Faghihi, S. *Biomed. Eng. Appl. Basis Commun.* **2013**, *26*, 145.
34. Karimi, A.; Navidbakhsh, M.; Faghihi, S.; Shojaei, A.; Hassani, K. *Proc. IMechE Part H: J. Eng. Med.* **2013**, *227*, 148.
35. Karimi, A.; Navidbakhsh, M.; Faghihi, S. Perfusion. doi: 10.1177/0267659113513823.
36. Fung, Y. *Am. J. Physiol.* **1967**, *213*, 1532.
37. Fung, Y. In Biomechanics, Its Foundations and Objectives; Fung, Y., Perrone, N., Anliker, M., Eds; Prentice-Hall: Englewood Cliffs, NJ, **1972**; p 181.
38. Kwan, M. K.; Lin, T. H. C.; Woo, S. L. Y. *J. Biomech.* **1993**, *26*, 447.
39. Lucas, S. R.; Bass, C. R.; Salzar, R. S.; Oyen, M. L.; Planchak, C.; Ziemba, A.; Shender, B. S. *Acta Biomater.* **2008**, *4*, 117.
40. Toms, S. R.; Dakin, G. J.; Lemons, J. E.; Eberhardt, A. W. *J. Biomech.* **2002**, *35*, 1411.
41. Troyer, K. L.; Puttlitz, C. M. *Acta Biomater.* **2011**, *7*, 700.
42. Lucas, S.; Bass, C.; Crandall, J.; Kent, R.; Shen, F.; Salzar, R. *Biomech. Model. Mechanobiol.* **2009**, *8*, 487.
43. Rajagopal, K. R.; Srinivasa, A. R.; Wineman, A. S. *Int. J. Plast.* **2007**, *23*, 1618.
44. Wang, Y.; Chen, L. *Carbohydr. Polym.* **2011**, *83*, 1937.
45. Corkhill, P. H.; Trevett, A. S.; Tighe, B. *J. Proc. IMechE Part H: J. Eng. Med.* **1990**, *204*, 147.
46. Tanaka, E.; van Eijden, T. *Crit. Rev. Oral Biol. Med.* **2003**, *14*, 138.
47. Allen, K. D.; Athanasiou, K. A. *J. Biomech.* **2006**, *39*, 312.
48. Tanaka, A.; Shibaguchi, T.; Tanaka, M.; Tanne, K. *J. Oral. Maxillofac. Surg.* **2000**, *58*, 997.
49. Chang, S. J.; Huang, Y.-T.; Yang, S.-C.; Kuo, S.-M.; Lee, M.-W. *Carbohydr. Polym.* **2012**, *88*, 684.
50. Ionita, M.; Pandele, M. A.; Iovu, H. *Carbohydr. Polym.* **2013**, *94*, 339.
51. Muliana, A.; Rajagopal, K. R. *Int. J. Solids Struct.* **2012**, *49*, 989.
52. Moore, J. E.; Soares, J. S.; Rajagapol, K. *Cardiovasc. Eng. Technol.* **2010**, *1*, 52.
53. Nekouzadeh, A.; Pryse, K. M.; Elson, E. L.; Genin, G. M. *J. Biomech.* **2007**, *40*, 3070.
54. Mirani, R. D.; Pratt, J.; Iyer, P.; Madihally, S. V. *Biomaterials* **2009**, *30*, 703.
55. Zhang, C.; Moore, I. *Polym. Eng. Sci.* **1997**, *37*, 414.
56. Craiem, D.; Rojo, F.; Atienza, J.; Armentano, R.; Guinea, G. *Phys. Med. Biol.* **2008**, *513*, 4543.
57. Sionkowska, A.; Płanecka, A. *J. Mol. Liq.* **2013**, *178*, 5.